

INTERROGATION AND ANALYSIS OF COMPLEX FUSION DECAY-HEAT BENCHMARK SIMULATIONS

Mark R. Gilbert¹ and Jean-Christophe Sublet^{2,1}

¹Culham Centre for Fusion Energy, United Kingdom Atomic Energy Authority,
Culham Science Centre, Abingdon, OX14 3DB, UK

²Nuclear Data Section, International Atomic Energy Agency,
P.O. Box 100, 1400 Vienna, Austria

mark.gilbert@ukaea.uk, j.c.sublet@iaea.org

ABSTRACT

Validation and verification (V&V) benchmark exercises form an important part of the development and release of the FISPACT-II inventory code and its associated input nuclear data libraries. This paper describes the latest V&V based on the fusion decay-heat measurements performed at the Japanese FNS facility. New and novel assessment techniques, focussed on the complex breakdown of decay-heat contributions from individual radionuclides, have been employed to interpret the simulated results, benchmark the data against the experimental measurements, and to compare results from different international nuclear data libraries. Example results are presented and discussed for the TENDL-2017, JEFF-3.3, ENDF/B-VIII.0, and legacy EAF2010 libraries, highlighting both good and poor predictive performance.

KEYWORDS: decay-heat benchmark, nuclear data validation, nuclear reactions, isomeric states, fusion neutrons

1. INTRODUCTION

There are several obstacles still to be surmounted to realise fusion as a future global energy source. A key issue concerns the choice and configuration of materials within a fusion reactor. Material performance at the engineering level under high neutron flux loads is a major concern. As well as the physical damage caused by the neutrons, fusion reactor operation must also be concerned with the transmutations caused by nuclear interactions. Changes in isotopic/chemical composition can influence material behaviour and performance as well as produce radioactive components. Radioactivity will constrain in time and cost the maintenance schedule during the lifetime of a power plant, as well as determining the economic and environmental implications of waste disposal. Accurate predictions of transmutation rates in neutron-irradiated materials is thus a key requirement for fusion power-plant planning and design. In the absence of a fusion experiment at the relevant power-plant scale, assessment of isotope composition evolution must rely on predictions from inventory simulations.

Inventory simulations, whereby the isotopic composition (the “inventory”) is evolved in-time under a specified neutron flux-energy distribution, are often accomplished by solving a matrix of coupled

differential equations that relate the rate-of-change of concentration N_i of each nuclide i to the (total) reaction cross sections that either destroy or create it:

$$\frac{dN_i}{dt} = \underbrace{-N_i(\lambda_i + \sigma_i\phi)}_{\text{destruction}} + \sum_{j \neq i} \underbrace{N_j(\lambda_{ji} + \sigma_{ji}\phi)}_{\text{creation}}, \quad (1)$$

where λ_i is the decay constant (in s^{-1} units) for nuclide i and σ_i in barns is the total cross section for all reaction that destroy it, which is typically evaluated by folding the normalized neutron flux spectrum with energy-dependent reaction cross sections. ϕ is the total neutron flux in $\text{n cm}^{-2} \text{s}^{-1}$, and the product $\sigma\phi$ is a per second reaction rate. λ_{ji} and σ_{ji} are the equivalent decay constants and total cross sections on all other nuclides j that create i .

FISPACT-II [1,2] is a world-leading code for calculating inventory evolution in materials. After several decades of ‘‘FISPACT’’ development, FISPACT-II has been re-engineered and modernized to take advantage of the latest international nuclear data libraries. This code has been thoroughly tested for robustness but accurate predictions from it rely on good quality nuclear data to feed it as input. Validation and verification exercises are used to test both the code and these nuclear databases. Several ‘‘benchmarks’’ have been developed for application to FISPACT-II, including an integro-differential validation [3], a fission decay-heat benchmark [4], and a comparison to high-energy, astrophysics data [5]. For the primary fusion objective of FISPACT-II a decay-heat benchmark has also been developed to compare simulated predictions with any nuclear data library to an extensive experimental database created by the Japan Atomic Energy Agency (JAEA) using their fusion neutron source (FNS) facility. The present paper focuses on this fusion-benchmark with a brief description of the original JAEA experimental method and the simulation process, followed by discussion of several of the code-vs-experiment comparisons from the latest version of the simulation benchmark [6]. These comparisons take advantage of the detailed interrogation techniques afforded by the FISPACT-II methodology, and highlight both proficiencies and deficiencies in international nuclear reaction data libraries.

2. Experimental procedure and simulation method

JAEA performed a series of experiments during the period 1996-2000 at the FNS facility [7,8,9]. More than 70 different materials (in thin, 10 μm thick, 25x25 mm^2 samples) were irradiated for either 5 minutes or 7 hours (or both) in the 14 MeV neutron source, where neutron fluxes were typically around $10^{10} \text{ n cm}^{-2} \text{ s}^{-1}$. After exposure, each sample was rapidly extracted (within 10 seconds for the short irradiations) to a Whole Energy Absorption Spectrometer (WEAS) where the decay-heat was measured at various time intervals as the material decay-cooled. The WEAS system provided almost 100% detection efficiency with very high sensitivity (down to a pico-Watt or less), allowing for the total experimental uncertainty to be less than 10% in most cases.

The reported data for the JAEA experiments [7] were very detailed, enabling the design of simulations to reproduce the experimental circumstances to be very robust and accurate. For each material a FISPACT-II simulation has been performed using all the experimental parameters: starting material composition (for some materials there were additional unknown errors associated with uncertainties in the chemical compositions of the samples); neutron flux spectrum (which varied

according to position in the FNS facility, but was well-defined otherwise using Monte-Carlo-based transport calculations); irradiation time; and experimental cooling times.

The simulation results have been compared to the corresponding experimental data via a specially designed set of automated analyses and visual representations. For each experiment, the simulation quality is judged using the following outputs (see [6,10] for more details):

1. Total decay-heat evolution plot: Curves for each data library simulation plotted as decay-heat (in μW) per g as a function of time after irradiation alongside the experimental decay-heat measurements (also measured per g). Experimental uncertainties (as vertical lines) and nuclear-data-derived uncertainties (as coloured bands in the plots).
2. Tabulated comparison at each experimental measurement: numerical comparison for each measurement time, including E/C (experiment over calculation) ratios.
3. Nuclide contributions graph: Simulated decay-heat broken-down into the individual radionuclide contributions (and compared against the experiment). These radionuclide-separated plots are a unique feature of FISPACT-II and allow complex inventories to be understood in a straightforward way [11]. A variation on these plots – where the nuclide contributions are plotted as % contributions to the total decay-heat (instead of the absolute decay-heat values of the former) – has also recently been developed [10] to simplify identification of the important radionuclides in the most complex cases (see later).
4. Tabulated nuclide uncertainties: characteristic E/C values and the associated uncertainties for each dominant nuclide that contributes more than 75% of the total decay-heat at any measured cooling time. This gives a numerical estimate of the likely uncertainty (both from the measurement and the simulation) associated with the predicted production of nuclides, and also indicates the accuracy with which the cross sections of production of a given nuclide are able to capture the experimental result.
5. Pathway analysis: tabulated primary production pathways for all the dominant nuclides (as evaluated by the standard use of FISPACT-II uncertainty keywords, UNCERT, LOOKA-HEAD, etc. – see [12]). Identifies the important reaction channels that were responsible for the dominant contributions to the simulated decay-heat.
6. decay-heat and half-lives plot: decay-heat plot showing the total decay-heat simulation curve and the important radionuclides labelled at the position of their heat level at shutdown in the simulations on the ordinate and half-life on the abscissa.

3. Typical results

The “FNS decay-heat” benchmark [6] has recently been performed for the TENDL-2017 [13], ENDF/B-VIII.0 [14], JEFF-3.3 [15], and fusion-specific EAF2010 [16] international data libraries. Example cases are discussed below to illustrate the complexity, subtlety and importance of the comparisons in this benchmark.

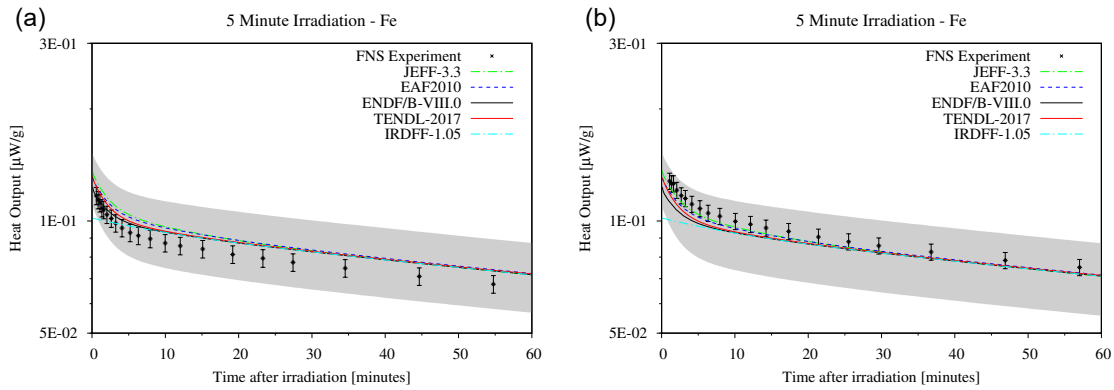


Figure 1: Simulated decay-heat comparisons to two different 5-minute irradiation experiments on iron samples at the FNS in Japan, performed in (a) 2000 and (b) 1996. Experimental data points are shown with uncertainties and the grey uncertainty band is associated with the TENDL-2017 simulation. Curves for four major international libraries (see the main text) are shown, as well as the FISPACT-II simulation curve obtained using the international dosimetry file IRDFF-1.05 [17]. While this library only contained a very small subset of the possible nuclear reactions, it is nonetheless suitable for validation against some of the FNS experiments - including iron.

3.1. Iron

Iron should be a trivial case – it is a well studied material (perhaps only uranium has received more attention) with a wealth of experimental measurements to support the evaluation of nuclear reaction cross sections. However, figure 1 shows that this is a case where the experimental results are problematic. The figure shows the experiment and code comparison for two separate 5-minute irradiations of iron at FNS – one performed in 1996, and the second 4 years later in 2000. The experimental set-up was identical in both cases, which is borne out by the equivalence of the simulation results in the two cases (the curves in the figure). However, instead of identical experimental measurements, there is significant deviation; one set of experimental decay-heats is above the simulation curves and one is below them. A possible culprit here is the presence of unknown impurities in one or other of the samples, but either way this example highlights that even in a carefully controlled experiment there can still be unknown sources of error. On the other hand, the simulated decay-heat curves nicely capture the experimental decay profile, implying a good match between the identified primary radionuclides in the simulation and the reality: the half-life of the main radionuclide – in this case ^{56}Mn [6] – determines the profile of the curves.

3.2. SS316

A better experimental case (and more typical for the high-quality experimental procedures) is illustrated by nuclide contribution charts in figure 2 for the TENDL-2017 benchmark against 7-hour irradiations of SS316 steel. Here there is near perfect agreement between simulation and experiment (the average % difference between experiment and simulation is only 6%), which is remarkable given the relative complexity shown in the simulation; there are many contributing

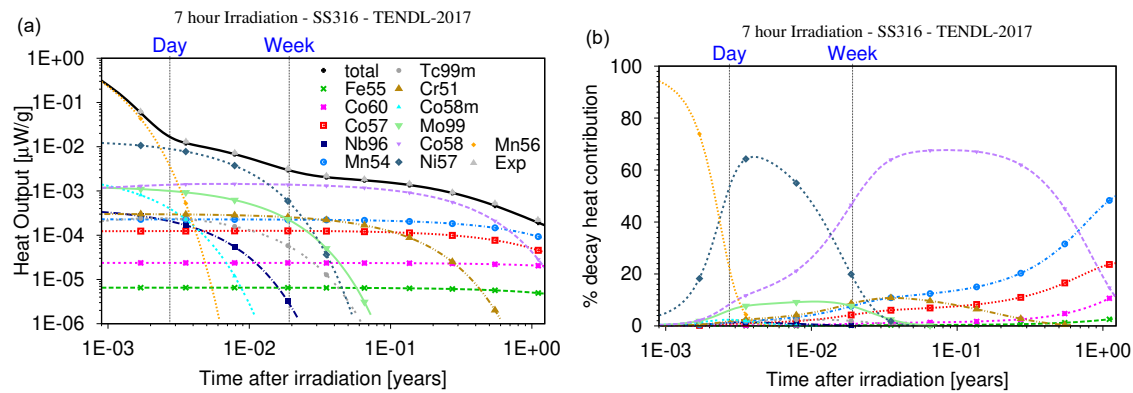


Figure 2: Decay-heat measurements and FISPACT-II-with-TENDL-2017 simulation of a 5-minute irradiated sample of SS316 steel. (a) shows the absolute simulated decay-heat curves for the main contributing radionuclides identified in the simulation. The “total” curve is the total decay-heat prediction from the simulation and the experimental measurements are shown as discrete points. (b) plots the % contributions to the total decay-heat for each nuclide as a function of time.

nuclides. The % contribution chart in figure 2b allows the dominant nuclides to be easily identified. The figures shows that three main radionuclides ^{56}Mn , ^{57}Ni , and ^{58}Co dominate the decay-heat at different times after the irradiation – at less than one day after irradiation, from 1 day to a few days, and from 1 week to almost a 10 months, respectively, for the three nuclides.

3.3. Tin

Cooling after the 7-hour irradiation experiment and simulation of tin (as an oxide SnO_2) is depicted in figure 3 as nuclide contribution graphs (both absolute decay-heat and % contributions) for FISPACT-II simulations with TENDL-2017 and JEFF-3.3. The two different libraries produce very different results: while TENDL-2017 predictions are a very good match to the experimental measurements, JEFF-3.3 under-predicts the decay-heat during the first 50 days of cooling. According to the TENDL-2017 simulation, during this time the heat is predominantly produced from the metastable ^{117m}Sn radionuclide, which JEFF-3.3 completely fails to predict. This short-lived nuclide ($T_{1/2} = 13.6$ days) comes mainly from (n,2n) reactions on ^{118}Sn (according to TENDL-2017). It seems that JEFF-3.3 has not properly apportioned this reaction channel between the metastable ^{117m}Sn and ground-state, stable ^{117}Sn .

3.4. Osmium and indium

The simulated decay-heat curves for the 5-minute irradiation of osmium shown in figure 4 are not close to the measured points. Even worse, there is very large variation between the different libraries, which makes it difficult to pinpoint the exact issue with the code predictions, or to assess the quality of the experiment. Analysis of the EAF2010 results suggest that the decay profile of ^{190m}Os ($T_{1/2} = 9.9$ minutes) is a good match to the measured profile and hence this radionuclide should dominate the simulated decay-heat. The other libraries don't currently generate this nuclide

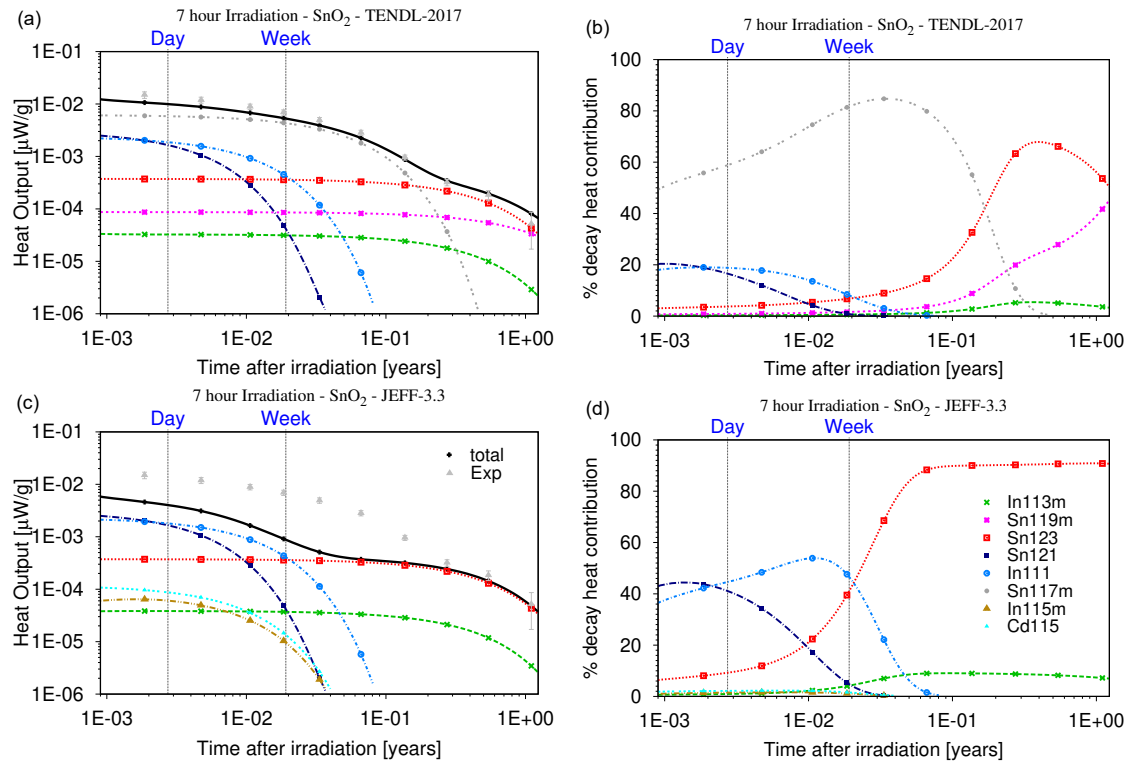


Figure 3: Simulated nuclide contributions to the decay-heat after 7-hour irradiation of tin-oxide with TENDL-2017 (a,b) and JEFF-3.3 (c,d) nuclear libraries. Absolute decay-heats (including simulated totals and experimental points) are shown in (a,c), while (b,d) show the time variation in % contributions from each radionuclide indicated in the legend (in (d)).

and all overpredict various other longer-lived metastable nuclides, producing the anomalous decay profiles shown. A recommendation for future library development would be to properly include the production of ^{190m}Os , which, according to the EAF2010 simulations, is via (n,n') reactions on ^{190}Os .

A similar situation occurs for the simulations of a 5-minute experiment on indium (figure 5). Once again, all the libraries fail to adequately predict the experimental result, and once more EAF2010 seems to show the best match to the measured decay profile (if not the absolute values). The EAF2010 simulations show dominance of ^{114}In at cooling times below 5 minutes, with ^{116m}In dominating the remaining experimental cooling times. Both are produced via reactions on ^{115}In – $(n,2n)$ and (n,γ) , respectively for 114 and 116m – and the combined decay profile of these two nuclides with their 1.2 and 54.6 minute half-lives, respectively, well captures the profile at the start and end of the experiment (figure 5b). However, the production of ^{116m}In is clearly overestimated, resulting in it dominating the ^{114}In decay-heat too soon in the simulation and in the total decay-heat being higher than the experimental measurements. Similarly, TENDL-2017 also overpredicts ^{116m}In production, but by an even larger amount, causing it to dominate the decay-heat at all cooling times and producing an incorrect profile at short timescales for this library in figure 5a as well as the extremely high decay-heat. Meanwhile, JEFF-3.3 and ENDF/B-VIII.0 completely

miss ^{116m}In production (but do predict the correct ^{114}In level – as all libraries seem to do), and thus misrepresent the majority of the experimental profile. A clear conclusion from this experimental comparison is the need for careful re-evaluation and guaranteed inclusion of the $^{115}\text{In}(n,\gamma)$ channel to all isomeric states of ^{116}In in future nuclear libraries.

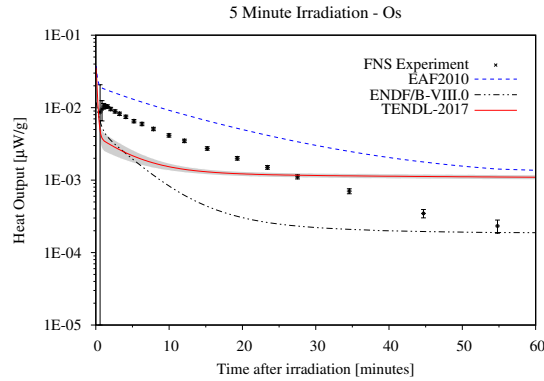


Figure 4: Decay-heat simulation vs. experiment comparison for a 5 minute irradiation of osmium. None of the different library simulations shown (JEFF-3.3 is identical to TENDL-2017) produce a good match to the experiment.

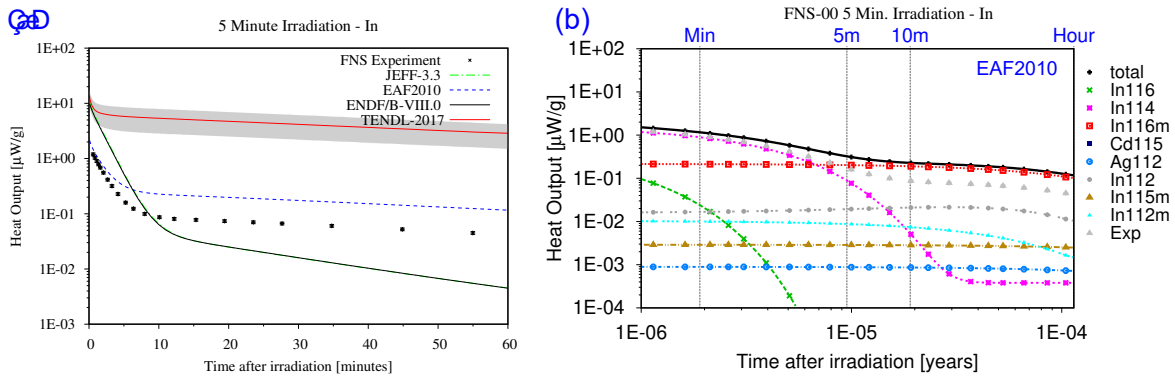


Figure 5: Decay-heat simulation vs. experiment comparison for a 5 minute irradiation of indium. The total decay-heat profiles in (a) show that none of the different library simulations (JEFF-3.3 is identical to ENDF/B-VIII.0) produce a good match to the experiment. (b) shows the radionuclide breakdown in the FISPACT-II simulations performed with EAF2010.

4. SUMMARY

Validation, verification, and benchmarking of nuclear codes and the underlying input nuclear physics data are necessary to prove the quality of predictions for nuclear systems. The fusion decay-heat benchmark discussed here is wide-ranging in its coverage of materials and specifically tests the suitability of nuclear cross section libraries to simulate material response under a 14 MeV-

peaked fusion spectrum. The benchmark has recently [6] been performed with the latest versions of the major international nuclear data libraries; TENDL-2017, JEFF-3.3, and ENDF/B-VIII.0.

Detailed analysis techniques have been developed to probe the subtleties in each individual measurement set; for example, graphical visualization of the time-evolving contributions to decay-heat from different radionuclides – a capability afforded by FISPACT-II’s detailed inventory outputs – offers new insight into the quality of the simulated decay profiles, both quantitatively and qualitatively. For many materials the major libraries produce a good match to the measurements, but for some important cases for some libraries (sometimes all) there is still a need for re-evaluation – perhaps guided by the better quality of predictions with older “legacy” libraries such as the EAF2010 database also considered in [6]. This integral benchmark test provides the evidence to justify alteration of appropriate differential cross section data.

ACKNOWLEDGEMENTS

This work was funded by the RCUK Energy Programme [grant number EP/P012450/1]. The work was also partly carried out within the framework of the EUROfusion Consortium and received funding from the Euratom research and training programme 2014-2018 under grant agreement No 633053. The views and opinions expressed herein do not necessarily reflect those of the European Commission. To obtain further information on the data and models underlying this paper please contact PublicationsManager@ukaea.uk.

REFERENCES

- [1] J.-Ch. Sublet, J. W. Eastwood, J. G. Morgan, M. R. Gilbert, M. Fleming, and W. Arter. “FISPACT-II: An Advanced Simulation System for Activation, Transmutation and Material Modelling.” *Nucl Data Sheets*, volume 139, pp. 77–137 (2017). <http://dx.doi.org/10.1016/j.nds.2017.01.002>.
- [2] “FISPACT-II, release 4.0.” (2018). <http://fispact.ukaea.uk>.
- [3] M. Fleming, J.-Ch. Sublet, and J. Kopecky. “Integro-Differential Verification and Validation, FISPACT-II & TENDL-2017 nuclear data libraries.” Technical Report UKAEA-R(18)004, UKAEA (2018). Available from <http://fispact.ukaea.uk>.
- [4] M. Fleming and J.-Ch. Sublet. “Validation of FISPACT-II decay heat and inventory predictions for fission events.” Technical Report UKAEA-R(18)003, UKAEA (2018). Available from <http://fispact.ukaea.uk>.
- [5] M. Fleming, J.-Ch. Sublet, A. Koning, and D. Rochman. “Maxwellian-Averaged Neutron-Induced Cross Sections for $kT=1$ keV to 100 keV, KADoNiS, TENDL-2014, ENDF/B-VII.1 and JENDL-4.0u nuclear data libraries.” Technical Report UKAEA-R(18)005, UKAEA (2018). Available from <http://fispact.ukaea.uk>.
- [6] M. R. Gilbert and J.-Ch. Sublet. “Fusion decay heat validation, FISPACT-II & TENDL-2017, EAF2010, ENDF/B-VIII.0, JEFF-3.3, and IRDFF-1.05 nuclear data libraries.” Technical Report CCFE-R(18)002, UKAEA (2018). Available from <http://fispact.ukaea/>.
- [7] F. Maekawa et al. Technical Report JAERI 99-055, JAERI-Data/Code 98-021, JAERI-Data/Code 98-024, JAEA (1999).

- [8] F. Maekawa, K. ichiro Shibata, M. Wada, Y. Ikeda, and H. Takeuchi. “Comprehensive Activation Experiment with 14-MeV Neutrons Covering Most of Naturally Existing Elements 5 Minutes Irradiation Experiment .” *J Nucl Sci Tech*, **volume 39**(sup2), pp. 990–993 (2002). <https://doi.org/10.1080/00223131.2002.10875267>.
- [9] F. Maekawa and Y. Ikeda. “Decay heat experiment on thirty-two fusion reactor relevant materials irradiated by 14-MeV neutrons.” *Fus Eng Des*, **volume 47**(4), pp. 377–388 (2000). [https://doi.org/10.1016/S0920-3796\(99\)00079-4](https://doi.org/10.1016/S0920-3796(99)00079-4).
- [10] M. R. Gilbert and J.-Ch. Sublet. “Experimental decay-heat simulation-benchmark for 14 MeV neutrons & complex inventory analysis with FISPACT-II.” *Nucl Fusion* (2019). <https://doi.org/10.1088/1741-4326/ab278a> in press.
- [11] M. R. Gilbert, M. Fleming, and J. -Ch. Sublet. “Inventory simulation tools: Separating nuclide contributions to radiological quantities.” *EPJ Web Conf*, **volume 146**, p. 09017 (2017). <https://doi.org/10.1051/epjconf/201714609017>.
- [12] M. Fleming, T. Stainer, and M. R. Gilbert. “The FISPACT-II User Manual.” Technical Report UKAEA-R(18)001, UKAEA (2018).
- [13] A. J. Koning and D. Rochman. “TENDL-2017.” (2017). Available from https://tendl.web.psi.ch/tendl_2017/tendl2017.html.
- [14] D. Brown, M. Chadwick, M. Herman, et al. “ENDF/B-VIII.0.” (2018). Available from <https://www.nndc.bnl.gov/endl/b8.0/index.html>.
- [15] “JEFF-3.3.” (2017). Available from <http://www.oecd-nea.org/dbdata/jeff33>.
- [16] J.-Ch. Sublet et al. “EAF2010.” (2010). Details at <http://www.ccf.ac.uk/EASY2007.aspx>.
- [17] A. Trkov et al. “IRDF-1.05.” (2014). Available from <https://www-nds.iaea.org/IRDF/>.